https://doi.org/10.5194/tc-2019-299
Preprint. Discussion started: 10 December 2019

The Cryosphere Discussions
Open Access
EGU

Brief communication: Arctic sea ice thickness internal variability and its changes under historical and anthropogenic forcing

Guillian Van Achter[1], Leandro Ponsoni[1], François Massonnet[1], Thierry Fichefet[1], and Vincent Legat[2]

[1]Georges Lemaitre Center for Earth and Climate Research, Earth and Life Institute, Université Catholique de Louvain.
[2]Institute of Mechanics, Materials and Civil Engineering, Applied Mechanics and Mathematics, Université catholique de Louvain.

Correspondence: Guillian Van Achter (guillian.vanachter@uclouvain.be)

Abstract. We use model simulations from the CESM1-CAM5-BGC-LE dataset to characterise the Arctic sea ice thickness internal variability both spatially and temporally. These properties, and their stationarity, are investigated in three different contexts: (1) constant, pre-industrial, (2) historical and (3) projected conditions. Spatial modes of variability show highly stationary patterns regardless of the forcing and mean state. A temporal analysis reveals two peaks of significant variability and despite a non-stationarity on short time-scales, they remain more or less stable until the first half of the 21st century, where they start to change once summer ice-free events occur, after 2050.

1 Introduction

In the recent decades, Arctic sea ice has retreated and thinned significantly (Notz and Stroeve, 2016). The annual mean Arctic sea ice extent has decreased by $\sim 2 \times 10^6$ km^2 between 1979 and 2016 (Onarheim *et al.*, 2018). An analysis combining US Navy submarine ice draft measurements and satellite altimeter data showed that the annual mean sea ice thickness over the Arctic Ocean at the end of the melt period decreased by 2 m between the pre-1990 submarine period (1958-1976) and the Cryosat-2 period (2011-2018) (Kwok, 2018). On long timescales (several decades or more), these retreat and thinning are projected to continue as greenhouse gas emissions are expected to rise. However, on shorter timescales (1-20 yr), internal climate variability, defined as the variability of the climate system that occurs in the absence of external forcing and caused by the system's chaotic nature, limits the predictability of climate (Deser *et al.*, 2014) and represents a major source of uncertainty for climate predictions (Deser *et al.*, 2012). In this context, greater knowledge of Arctic sea ice thickness internal variability and of its drivers are both essential to document the true evolution of the atmosphere–ice–ocean system and to predict its future changes.

The mean spatial distribution of the Arctic sea ice thickness is relatively well documented (Stroeve *et al.*, 2014). But there are some uncertainties around its interannual variability and its spatial modes of variability. Some studies (Singarayer and Bamber, 2003; Lindsay and Zhang, 2006; Fuckar *et al.*, 2016) already analysed the spatial distribution of Arctic sea ice variability by applying empirical orthogonal functions (EOF) (K-means cluster analysis for Fuckar *et al.*, 2016) to historical sea ice thickness time series. They reported that the first mode is nearly basinwide, while the second and third ones are orthogonal lateral

https://doi.org/10.5194/tc-2019-299
Preprint. Discussion started: 10 December 2019

modes accounting for 30, 18 and 15% of the variability, respectively. The temporal sea ice volume variability has been studied by Olonscheck and Notz (2017). They enlightened a rather stable internal variability of annual sea ice volume and area for the historical climate compared to the pre-industrial one and an extremely likely decreased internal variability of winter and summer Arctic sea ice volume for a future climate forced by the RCP8.5 scenario.

Most of the studies cited above used data covering a few decades under historical forcing. In this work we use a long climate model control run under pre-industrial conditions, which enables us to study only the internal variability of the Arctic sea ice thickness. We study the internal variability both temporally and spatially by applying a wavelet analysis and an EOF decomposition to the Arctic sea ice volume and thickness anomaly time series, respectively. We also determine whether or not the sea ice volume and thickness variability is stationary by analysing the model outputs under historical and future climate conditions.

This manuscript is organised as follows. The model and its outputs are briefly described in Section 2. In Section 3, the spatial and temporal internal variability of Arctic sea ice are analysed, as well as their persistence through historical and future climate conditions. Then we explore the drivers of the main modes of internal variability. Conclusions are finally given in Section 4.

2 Data and methods

2.1 Sea ice thickness and volume datasets

We use the CESM1-CAM5-BGC-LE dataset (Kay *et al*., 2015). The Community Earth System Model Large Ensemble (CESM-LE) was designed to both disentangle model errors from internal climate variability and enable the assessment of recent past and future climate changes in the presence of internal climate variability. The CESM1(CAM5) model consists of coupled atmosphere, ocean, land and sea ice component models. It also includes a representation of the land carbon cycle, diagnostic biogeochemistry calculations for the ocean ecosystem and a model of the atmospheric carbon dioxide cycle (Moore *et al*., 2013; Lindsay *et al*., 2014). Jahn *et al*. (2016) showed good agreement between observations and CESM1(CAM5) simulations for mean Arctic sea ice thickness and extent in the early twenty-first century, and Barnhart *et al*. (2016) demonstrated that CESM1(CAM5) captures the trend of declining Arctic sea ice extent over the period of satellite observations. Based on these validation studies, it can be assumed that the CESM1-CAM5-BGC-LE time series is an adequate proxy to study the variability of Arctic sea ice thickness under different conditions. The dataset contains 3 main simulations. The first one is a 1700-yr control simulation with constant pre-industrial forcing. The ocean model was initialised from a state of rest (Danabasoglu *et al*., 2012), while the atmosphere, land and sea ice models were initialised using previous CESM1(CAM5) simulations. This experimental design allows the assessment of internal climate variability in the absence of climate change. The two other simulations are a historical (1850-2005) simulation and a future climate simulation (2006-2100) following the representative concentration pathway (RCP) 8.5 scenario, corresponding to a total radiative forcing of 8.5 W/m^2 in 2100 relative to pre-industrial conditions (Meinshausen *et al*., 2011). The Canadian Archipelago region was removed from the dataset due to sea ice thickness reaching

https://doi.org/10.5194/tc-2019-299
Preprint. Discussion started: 10 December 2019

unrealistic values in this area.

In this paper, we use the monthly averaged Arctic sea ice thicknesses (SIT) provided over the 3 periods (pre-industrial, historical and future). The variability analysis is applied on the SIT and sea ice volume (SIV) anomaly time series. The trend and seasonal cycle are removed to focus on the long-term variability. The anomaly is calculated in three steps. For each month, we build a time series with all values of that month over the entire period. Then, we compute the second degree polynomial fitting the time series. Finally, we remove that polynomial fitting from the original time series. Repeating those steps for each month, we get the original time series without the trend and seasonal cycle.

2.2 Variability analysis

In order to characterise the internal variability of the Arctic SIT, we aim at inspecting how it evolves over time and whether there are regions marked by different variabilities. Usual spectral analyses assume stationary of the time series. Having no certainty about the stationary character of the SIV time series even over long periods, we performed the analysis of the temporal variability of the SIV time series by means of wavelet analysis following the methodology proposed by Torrence and Compo (1998). The wavelet analysis is appropriate for non-stationary time series. It determines the evolution of periodicities in the time-space and provides higher resolution in the periodicity (Soon et al. 2011). The wavelet analysis is applied to the SIV anomaly time series under pre-industrial (200-years), historical (1850-2005) and future (2006-2100) conditions.

The spatial variability is analysed by computing the EOFs on the SIT anomaly time series as conducted by Lindsay and Zhang (2006). This decomposition reduces the large number of variables of the original data to a few variables, but without compromising much of the explained variance. Each EOF represents a mode of SIT variability that provides a simplified representation of the state of the SIT at that time along that EOF. In other words, the EOFs themselves are fixed in time but their weighting coefficients are time-varying; the associated time series (one for each mode) indicate in which state the SIT is at any time (Hannachi, 2004). The analysis is made on the gridded SIT anomaly time series, over the same periods as defined for the temporal analysis, except for the future climate period which spans from 2006 to 2050 (reasons are given in Section 3.1).

By applying the analysis separately over the 3 periods we aim to document the internal variability in the absence of any external forcing during the pre-industrial period and estimate the evolution of the SIT internal variability under anthropogenic forcing, by comparing the pre-industrial results with those for the historical and future periods.

https://doi.org/10.5194/tc-2019-299
Preprint. Discussion started: 10 December 2019


The Cryosphere Discussions

3 Results

3.1 Temporal variability

The results from the wavelet analysis are presented in Figure 1, in which the global wavelet spectrum is shown as a function of time (bottom-left of each subfigure). The time-integrated wavelet spectrum is also shown (bottom-right), which is a time-integrated power of the global wavelet spectrum. The significance level of the time-integrated wavelet spectrum is indicated by the dashed curve; it refers to the power of the red noise level at the 95% confidence level that increases with decreasing frequency.

The temporal variability of the Arctic SIV anomaly over the pre-industrial period is depicted in Figure 1a. The time-integrated power spectrum (bottom-right) shows 2 peaks of significant variability. The first peak corresponds to a period centered on 8 years but spanning from 5 to 10 years. The second one corresponds to a period of 16 years spanning from 10 to 20 years. Another peak, presenting a periodicity of 42 years, is present but not taken into account since the peak is below the significance level. The wavelet power spectrum is presented in the bottom-left panel of Figure 1a, in which the significant variability is highlighted by the regions enclosed by the yellow line. Two first peaks are present throughout the period, but they do not appear together at the same time. Depending on the time, either the 8- or 16-years peak is the dominant peak. For instance, the 8-years peak is dominant during the 1780-1810 and 1825-1840 periods, and the 16-years peak during the 1750-1790 and 1830-1850 periods.

Over the historical period, the Arctic SIV temporal variability shows a first peak centered on 5 years and two others centered on 10 and 16 years, all with 95% reliability. Regarding the wavelet power spectrum, it exhibits a constant line of variability at 16 years and another one, but less constant over the whole period, at 8 years. Those peaks and bands of variability are shown in Figure 1b. The future climate SIV wavelet analysis in Figure 1c presents a clear loss of variability after the year 2050. This loss of variability is visible in the SIV time series and is confirmed by both the wavelet power spectrum and the time-integrated power spectrum. The 2050 sudden loss of variability coincides with the ice-free summer events occurring at that time. Apart from that loss of variability, the wavelet power spectrum exhibits one band of 5-years variability during the 2010-2025 period and another band of 16-years variability during the 2025-2050 period, both bands with 95% of confidence.

https://doi.org/10.5194/tc-2019-299
Preprint. Discussion started: 10 December 2019

The Cryosphere Discussions
Open Access
EGU

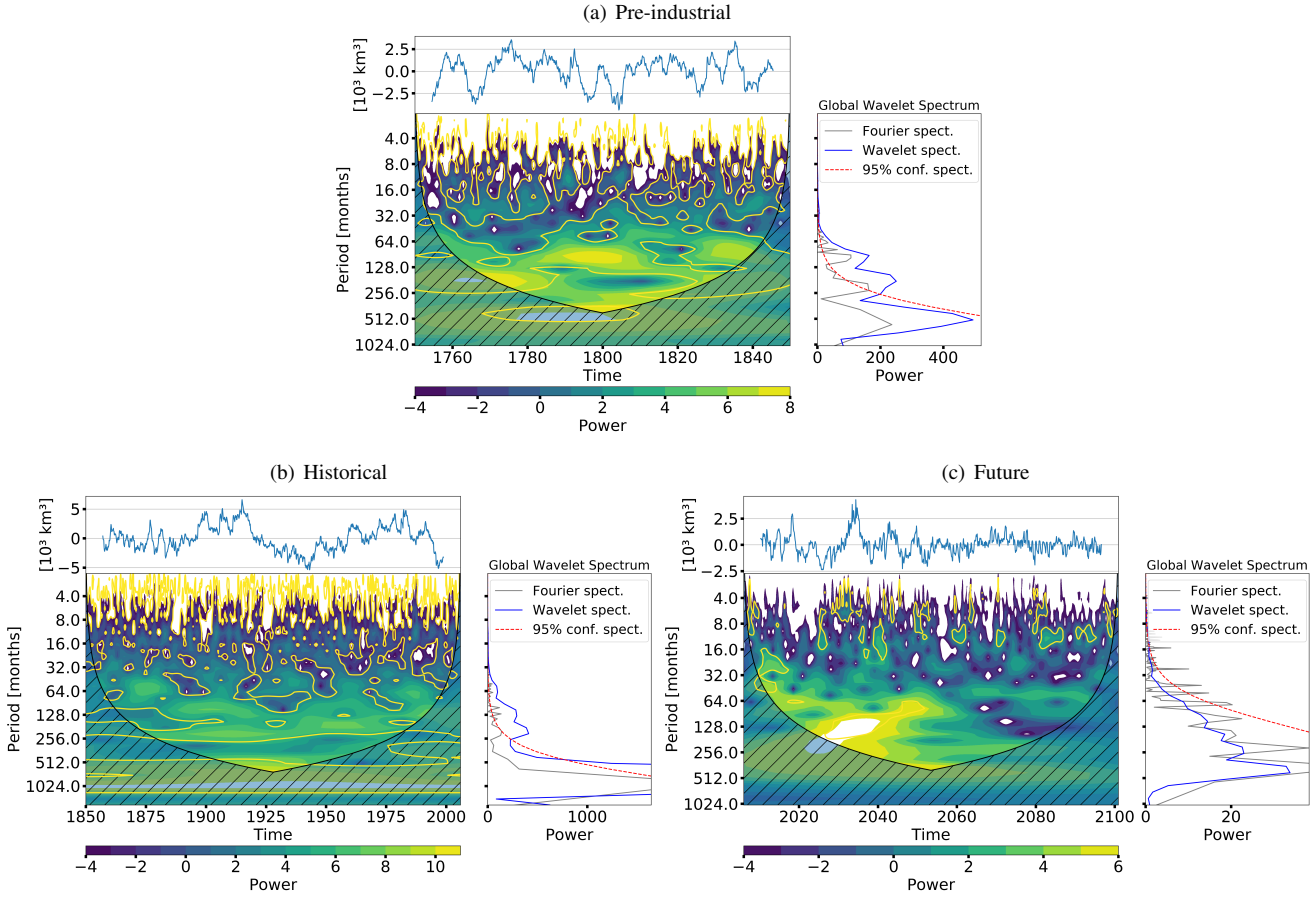

Figure 1. Wavelet analysis, with Morlet as the mother wavelet, applied to the Arctic sea ice volume anomaly over pre-industrial (a), historical (b) and future (c) periods. Each of the subfigure (a-c) presents sea ice volume anomaly time series (top), the wavelet power spectrum (bottom-left) and the time-integrated power spectrum from the wavelet analysis (bottom-right).

The main characteristics of the temporal variability of the Arctic SIV under pre-industrial conditions seems to persist under anthopogenic forcing. The two main temporal peaks of variability centered on 8 years and 16 years, found in the pre-industrial run, are present as band of variability in the power spectrum or peak of variability in the wavelet spectrum in both the historical period and the first half of the 21st century. Furthermore, the SIV variability seems to be non-stationary. Indeed, for a certain period, the main periodicity of the SIV variability can be either centered on 8 or 16 years.

3.2 Spatial variability

The spatial variability of the Arctic SIT anomaly is depicted by the major modes of variability in Figure 2. For each period, the modes are sorted by percentage of variability explained. The first mode, which explains most of the variability, represents 22, 19 and 20 % of the variability for pre-industrial, historical and future climate conditions, respectively. All periods show

https://doi.org/10.5194/tc-2019-299
Preprint. Discussion started: 10 December 2019

the same pattern of SIT spatial variability for the first mode. It corresponds to a dipole between the Fram Strait area and the East Siberian Sea (Figure 2 (a,b,c)). For both the pre-industrial and historical periods, the second mode of variability is a pole centered in the East Siberian Sea and spreading into the Arctic Basin (Figure 2 (d,e)). It accounts for 14 and 17 % of the variability, respectively. The third mode of variability for the pre-industrial period corresponds to a dipole between the Laptev and Kara Seas, on the one hand, and the east coast of Greenland, the Chukchi and Beaufort Seas on the other hand.

The first mode of SIT is stable over time and stays the dominant mode of spatial variability in all three periods. The disparities in percentage explained and in magnitude are few and some of them can be related to the length of the time series. As the first mode, the second mode of SIT spatial variability is persistent in both the pre-industrial and historical periods, but not in the future climate period. Indeed, the second mode of SIT variability under future climate conditions presents a pole of variability centered in the Arctic Basin, but regions of highest variability are close to the Canadian Archipelago and not in the East Siberian Sea, as it is the case for the second mode of the pre-industrial and historical periods. The third modes of the three periods exhibit all different patterns of variability and we are not going to use them in the following analysis.

https://doi.org/10.5194/tc-2019-299
Preprint. Discussion started: 10 December 2019

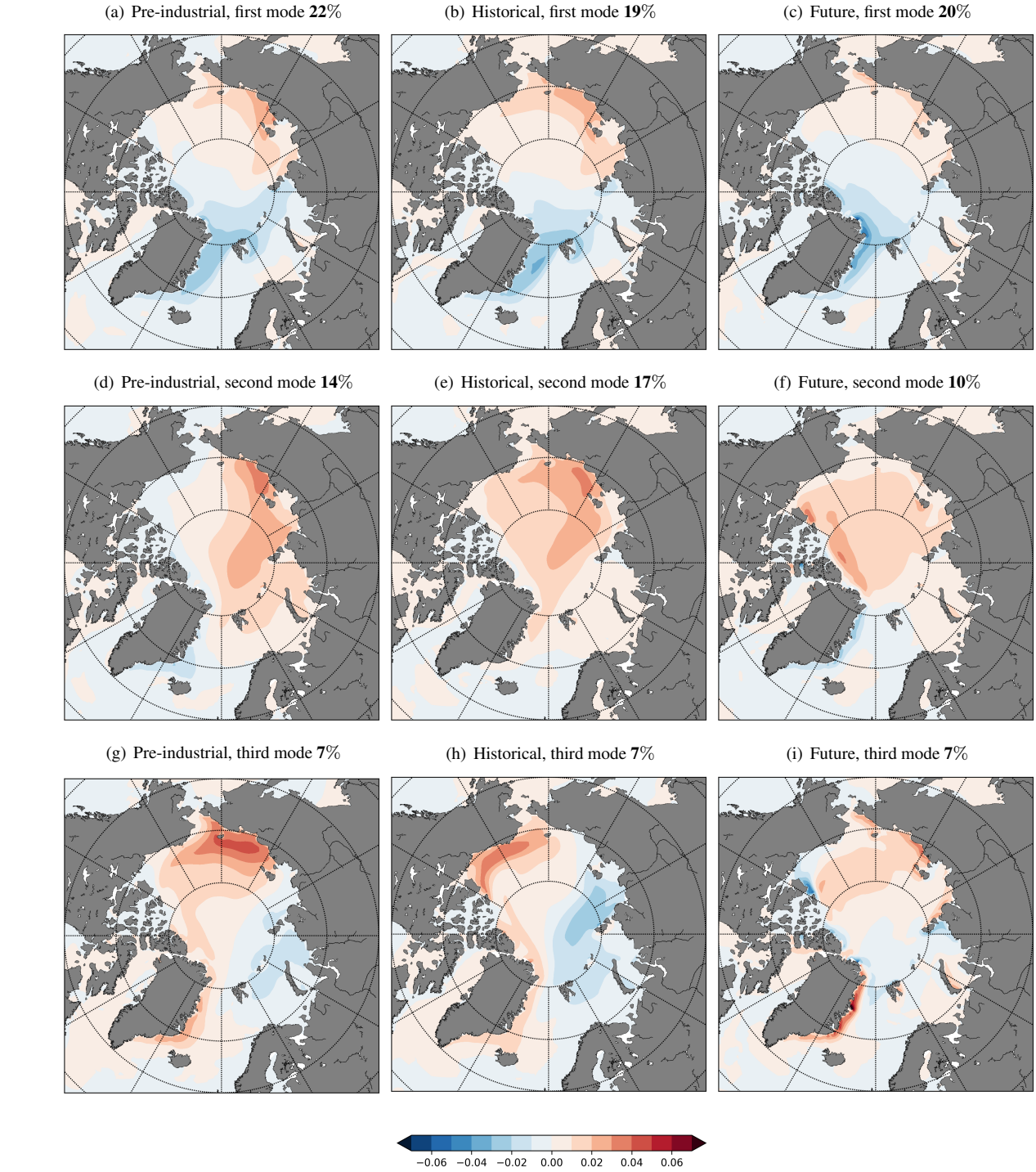

Figure 2. Modes of Arctic SIT spatial variability. From the left to the right, each row shows the three first EOF of Arctic SIT over the pre-industrial (a,d,g), historical (b,e,h) and future (c,f,i) periods, respectively.

https://doi.org/10.5194/tc-2019-299
Preprint. Discussion started: 10 December 2019

3.3 Drivers of the major modes of SIT internal variability

By computing the temporal oscillation between phases of a certain mode of variability, we are able to characterise this mode by low and high indices. In order to find the physical drivers of the SIT modes of variability, we investigate the differences in dynamic and thermodynamic features (sea ice velocity, atmospheric surface temperature) between both phases of the modes.
140 We looked at the mean sea ice circulation for each phase. Figure 3 shows the Arctic mean sea ice circulation over the pre-industrial period by compositing the low (a) and high (b) indices for the first mode of SIT variability. The sea ice drift anomaly associated with the positive and negative phases of the first SIT mode share similar features with the Arctic Oscillation: a cyclonic anomaly in the Beaufort Gyre, impacting the Transpolar Drift Stream, the Laptev Sea Gyre and the East Siberian circulation, as described by Rigor *et al*., (2002).
145

Furthermore, applying wavelet analysis to the associated time series of the first spatial mode of variability indicates that the main periodicity of this mode is centered on 8 years and spans from 5 to 10 years (not shown). This result allows us to link the first mode of temporal variability of the wavelet analysis to the first mode of spatial variability, and so, to the Arctic Oscillation.

150 We also used the associated time series of the second mode of SIT spatial variability to characterise it by low and high indices. Following Olonscheck *et al*. (2019) results, which demonstrate that the internal variability of Arctic sea ice area and concentration are primarily caused by atmospheric temperature fluctuations, we investigated the differences in mean surface air temperature anomaly over the pre-industrial period between the low (a) and high (b) indices of the second mode of SIT variability (see Figure 3). Two widely different states of surface air temperature are found. When the index of the mode of
155 variability is low, the surface air temperature is about 8°C lower than on average over the eastern side of the Arctic Basin. When the index is high, the center and western side of the Arctic Basin are on average colder by 8°C. Those strong discrepancies in mean surface air temperature, characterised by a cooling in the East Siberian, Laptev and Kara Seas in low phase or a cooling in the center and the western side of the Arctic Basin, are then causing strong variability in the SIT over the Arctic Basin through enhanced thermodynamic ice growth.
160

https://doi.org/10.5194/tc-2019-299
Preprint. Discussion started: 10 December 2019

The Cryosphere Discussions
Open Access
EGU

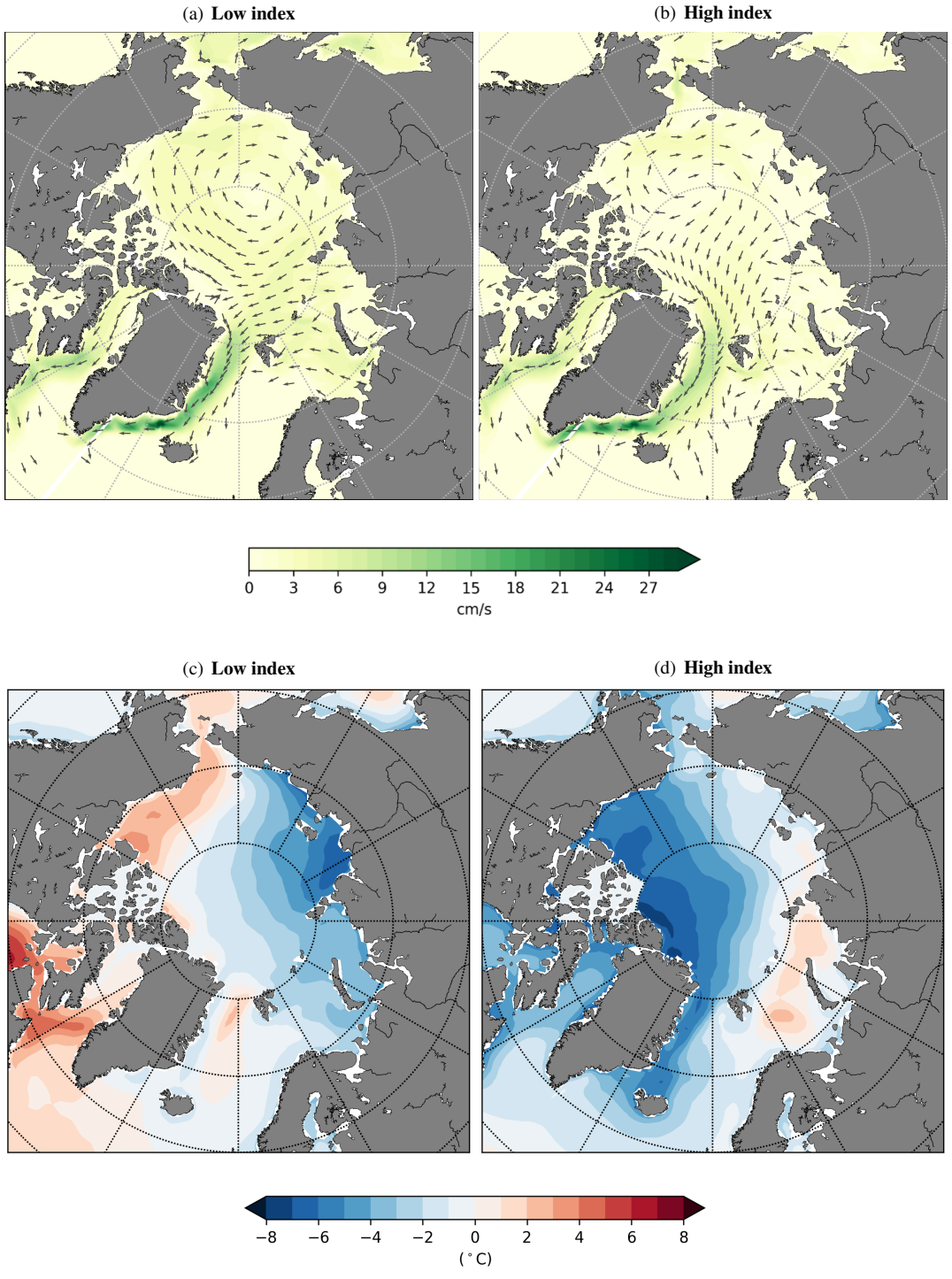

Figure 3. Arctic sea ice mean circulation during low (a) and high (b) indices of the first mode of SIT variability during the pre-industrial period. Arctic mean surface air temperature anomaly during low (c) and high (d) indices of the second mode of SIT variability.

https://doi.org/10.5194/tc-2019-299
Preprint. Discussion started: 10 December 2019

4 Conclusions

In this work, we have analysed the internal variability of the Arctic SIT both spatially and temporally with the CESM1-CAM5-BGC-LE dataset. We conducted a wavelet analysis of the SIV anomaly and an EOF decomposition of the SIT anomaly, both over a 200-yr control run conducted under pre-industrial conditions. Then, to assess the persistence of the SIT anomaly internal variability under anthropogenic forcing, we performed the same analyses over the 1850-2005 historical period and the future (2006-2050 for EOF and 2006-2100 for the wavelet analysis).

The temporal analysis of the SIV anomaly internal variability shows 2 peaks of significant variability. One centered on 8 years, spanning from 5 to 10 years, and another one centered on 16 years, spanning from 10 to 20 years. These two peaks of temporal variability are present in both the pre-industrial and historical periods, as well as in the first half of the 21 century. After that, a sudden loss of variability due to ice-free summer events is found. Furthermore, despite a dominant periodicity over the three periods, the SIV anomaly has been observed to be non-stationary. Indeed, the dominant periodicity of the SIV variability can be either centered on 8 or 16 years, depending on the timescale and period.

The spatial analysis of the SIT anomaly internal variability reveals two important modes of variability. The first one is a mode with opposite signs centered in the East Siberian Sea and in the Fram Strait area, accounting for 22% of the variability in the pre-industrial period. This first mode is a dynamical one, related to the Arctic Oscillation, and persists over all pre-industrial, historical and future periods. Furthermore, this first mode of spatial variability has a temporal variability of 8 years (spanning from 5 to 10 years), corresponding to the first peak of variability found in the temporal analysis. The second mode exhibits a large pole of variation centered on the East Siberian Sea going through the Arctic Basin. It represents 14% of the variability in the pre-industrial period. It is a thermodynamic mode, which is linked to a variation in surface air temperature. This second mode of spatial variability is present in both the pre-industrial and historical periods.

The loss of sea ice in summer starting in 2050 and the strong decrease in SIV going from 15 to 10×10^3 km^3 in winter during the second half of the 21st century modifies strongly the variability of the ice both spatially and temporally. The main modes of spatial variability lose their significance or just disappear after 2050, and the temporal analysis shows a total disappearance of the variability at that time.

This analysis of the Arctic SIT and SIV variability bears some limits. Indeed, our results for the temporal and spatial patterns of variability are based on only one model, and despite a reasonable validation against observations, the model is not perfect. Other studies with other model outputs are therefore needed to confirm our conclusion.

Finally, in the context of recent climate changes, predicting sea ice has never been so important. Therefore, our analysis of the Arctic SIT and SIV internal variability could lead to better mooring and observing devices, able to improve our day-to-day

https://doi.org/10.5194/tc-2019-299
Preprint. Discussion started: 10 December 2019

observation of Arctic sea ice thickness and volume data, which are not as well documented as the sea ice extent or sea ice area.

Data availability. Data can be downloaded from the following source:
https://www.earthsystemgrid.org/dataset/ucar.cgd.ccsm4.CESM_CAM5_BGC_LE.ice.proc.monthly_ave.html.

Competing interests. The authors declare that they have no conflict of interest.

Acknowledgements. The work presented in this paper has received funding from the European Union's Horizon 2020 Research and Innovation programme under grant agreement no. 727862: APPLICATE project (Advanced prediction in Polar regions and beyond). François Massonnet and Leandro Ponsoni are F.R.S.-FNRS PostDoc and Research Associate, respectively. The dataset used in this study was made available by CESM Community.

https://doi.org/10.5194/tc-2019-299
Preprint. Discussion started: 10 December 2019

References

Barnhart, K. R., Miller, C. M., Overeem, I., and Kay, E.:Mapping the future expansion of Arctic open water, Nature Clim Change, 6, 280–285, doi: 10.1038/NCLIMATE2848, 2016.

Deser, C., Philips, A. S., Alexander, M. A., and Smoliak, B. V.:Projecting North American Climate over the Next 50 Years: Uncertainty due to Internal Variability, Journal of Climate, 27, 2271-2296, doi.org/10.1175/JCLI-D-13-00451.1, 2014.

Deser, C., Philips, A., Bourdette, V., and Teng, H.:Uncertainty in climate change projections: the role of internal variability, Climate Dynamics, 38, 527–546, doi.org/10.1007/s00382-010-0977-x, 2012.

Fučkar, N. S., Guemas, V., Johnson, N. C., Massonnet, F., and Doblas-Reyes, F.: Clusters of Interannual Sea Ice Variability in the Northern Hemisphere, Climate Dynamics, 47, 1527–1543, doi.org/10.1007/s00382-015-2917-2, 2016.

Hannachi, A.:A Primer for EOF Analysis of Climate Data, Department of Meteorology, University of Reading Reading, 2004.

Jahn, A., Kay, J. E., Holland, M. M., and Hall, D. M.:How predictable is the timing of a summer ice-free Arctic?, Geophys. Res.Lett., 43, 9113–9120, doi:10.1002/2016GL070067, 2016.

Kay, J.E., Deser, C., Phillips, A., Mai, A., Hannay, C., Strand, G., Arblaster, J.M., Bates, S.C., Danabasasoglu, D., Edwards, J., Holland, M., Kushner, P., Lamarque, J.-F., Lawrence, D. , Lindsay, K., Midd Leton, A., Munoz, E., Neale, E., Oleson, K., Polvani, L., and Vertenstein, M.:The Community Earth System Model (CESM) Large Ensemble Project, A Community Resource for Studying Climate Change in the Presence of Internal Climate Variability, American Meteorological society, 1333-1349, doi.org/10.1175/BAMS-D-13-00255.1, 2015.

Kwok, R.:Arctic sea ice thickness, volume, and multiyear ice coverage: losses and coupled variability (1958–2018), Environ. Res. Lett., 13, 10, https://doi.org/10.1088/1748-9326/aae3ec, 2018.

Lindsay, K., Bonan, G. B., Doney, S. C., Hoffman, F. M., Lawrence, D. M., Long, M. C., Mahowald, N. M., Moore, J. K., Randerson, J. T., and Thornton, P. E.:Preindustrial-control and twentieth-century carbon cycle experiments with the Earth system model CESM1(BGC), J. Climate, 27, 8981-9005, doi.org/10.1175/JCLI-D-12-00565.1, 2014.

Lindsay, R. W., and Zhang, J.: Arctic Ocean Ice Thickness: Modes of variability and the Best Locations from Which to Monitor Them, Journal of physical oceanography, 36, 496-506, doi.org/10.1175/JPO2861.1, 2006.

Meinshausen, M., Calvin, S. J., Daniel, J. S., Kainuma, M. L. T., Lamarque, J-F., Matsumoto, K., and Montzka, S. A.:The RCP greenhouse gas concentrations and their extensions from 1765 to 2300, Climatic Change, 109-213, doi.org/10.1007/s10584-011-0156-z, 2011.

Moore, C. P., Lindsay, K., Doney, S. C., Long, S. C., and Misumi, K.:Marine ecosystem dynamics and biogeochemical cycling in the Community Earth System Model[CESM1(BGC)]:Comparison of the 1990s with the 2090s under the RCP4.5 and RCP8.5 scenarios, J. Climate, 26, 9291-9312, doi.org/10.1029/2011JD017187, 2013.

Notz, D., and Stroeve, J.:Observed Arctic sea-ice loss directly follows anthropogenic CO2 emission, Science, 354, 747-750, doi: 10.1126/science.aag2345, 2016.

Olonscheck, D., Mauritsen, T., and Notz, D.: Arctic Sea-Ice Variability Is Primarily Driven by Atmospheric Temperature Fluctuations, Nature Geoscience, 12, 6, 430–34, doi.org/10.1038/s41561-019-0363-1, 2019.

Olonscheck, D., and Notz, D.: Consistently estimating internal climate variability from climate-model simulations, J. Climate, 30, 9555-9573, doi:10.1175/JCLI-D-16-0428.1, 2017.

Onarheim, I. H., Eldevik, T., Smedsrud, L. H., and Stroeve, J. C.: Seasonal and Regional Manifestation of Arctic Sea Ice Loss, J. Climate, 31, 4917–4932, https://doi.org/10.1175/JCLI-D-17-0427.1, 2018.

https://doi.org/10.5194/tc-2019-299
Preprint. Discussion started: 10 December 2019

240 Rigor, I. G., Wallace, J. M., and Colony, R. L.:Response of Sea Ice to the Arctic Oscillation, Journal of Climate, 15, 2648, doi.org/10.1175/1520-0442(2002)015<2648:ROSITT>2.0.CO;2, 2002.

Singarayer, J. S., and Bamber, J. L.:EOF analysis of three records of sea-ice concentration spanning the last thirty years, Geophys. Res. Lett, 30, 1251, doi.org/10.1029/2002GL016640, 2003.

Soon, W., Dutta, K., Legates, D. R., Velasco, V., and Zhang, W. J.: Variation in surface air temperature of China during the 20th century,
245 Journal of Atmospheric and Solar-Terrestrial Physics, 73, 2331-2344, doi:10.1016/j.jastp.2011.07.007, 2011.

Stroeve, J., Barrett, A., Serreze, M., and Schweiger, A.: Using records from submarine, aircraft and satellites to evaluate climate model simulations of Arctic sea ice thickness, The Cryosphere, 8, 1839-1854, doi.org/10.5194/tc-8-1839-2014, 2014.